Experimental study of a vane-type pipe separator for oil–water separation

Shi Shi-ying, Xu Jing-yu, Sun Huan-qiang, Zhang Jian, Li Dong-hui, Wu Ying-xiang*

Institute of Mechanics, Chinese Academy of Sciences, Beijing 100190, China

ABSTRACT

An experimental study of a new vane-type pipe separator (VTPS) was conducted for the possible application in the well-bore for oil–water separation and reinjection. Results by using particle image velocimetry (PIV) reveal a better flow field distribution for oil–water separation, which is formed in VTPS than that in hydrocyclone. The effects of split ratio, the oil content, guide vanes' installation and number of guide vanes on oil–water separation performance have been investigated experimentally. Compared to a traditional single hydrocyclone, VTPS shows a good separation performance as the water content at the inlet of VTPS reaches 79.9%, the oil content at the water-rich outlet is about 400 ppm while the split is near 0.70. These results are helpful to provide a possibly new design for downhole oil–water separation.

1. Introduction

When the produced water in mature oil fields continues to increase, it is of great significance to separate the ever-increasing volumes of water from oil downhole and inject it into a suitable formation. The adoption of these measures could not only extend the economic exploitation of oil fields, but also maintain the reservoir pressure (Chapuis et al., 1999).

The mentioned process is attractive but needs further investigation about the structure optimization of separator for the limited space in the well-bore. Traditional downhole separator is hydrocyclone which is a kind of tangential inlet structure combining with a long small cone tail and an upflow tube (Ogunsina and Wiggins, 2005). According to the number of tangential inlets, traditional hydrocyclone could be classified into two types: "multi-inlet" (Jiang et al., 2002) and "single-entry". While due to the well-bore's small diameter, hydrocyclone with a single-entry is chosen in most cases (Bowers et al., 1999). According to information on the downhole hydrocyclone installations in North America, it works in wells' diameter larger than 135 mm with water content of greater than 88.4% (Veil et al., 1999). These downhole applications present the limitation of hydrocyclone and there is not much experience with hydrocylone used on streams with high oil content as well. These restrictions are mainly due to the shortcomings of hydrocyclone's entry. The "single-entry" caused by the limited space is always small. Small inlets are more likely to cause oil droplets break-up (Listewnik, 1984) and thus exacerbate the difficulties of oil–water separation process (Meyer and Bohnet, 2003). Besides, the "single-entry" makes the structure of hydrocyclone asymmetric and so does the flow field which would cause the oil core start to weave, oscillate (Schutz et al., 2009) and re-mixing of oil droplets between the oil core and water to happen (Thew, 1986). If the oil phase is re-emulsified, it would be quite difficult to separate oil droplets from water and even lead to the presence of some oil droplets in water injected to a disposal zone. The potential problems of this lasting oily-water stream reinjection will add to the difficulties in subsurface injection of the produced liquid (van den Broek et al., 2001) and reduce the field oil production. To solve the above problems, Sooran et al. tried to improve the separation efficiency through the redesign of inlet structures. Michdet and Sangesland (1996) studied hydrocyclones with a small tube inside the underflow tube so as to recollect the oil phase in the underflow. However the quantity of water-removal would be lowered considering the fact that the underflow tube of hydrocyclone is already very small. Klasson et al. (2005) and Zhao et al. (2010) presented a new method

---

Fig. 1 – Schematic of VTPS.

Table 1 – Designs of different guide vanes for experiments.			
θ	20°	30°	40°
n	3	2, 3, 4	3

tangentially inlet is always 0.14–0.17 times that of the cylinder so that the distance of an oil droplet moves from the inlet to the cylinder axis is short on the assumption of the same area of the cylinder's cross-section. This would shorten the time of the oil-droplet to move into the central area and increase the separation efficiency; Thirdly, in the VTPS, no reverse flow exists as well as no change in axial direction of flow between centrosymmetrical oil-core and the water phase near the wall. This reduces the risk of remix between the oil-core and surrounding water phase and help to promote the separation efficiency.

2. Experimental

2.1. Experimental setup and operation principle

An experimental flow loop has been constructed and shown in Fig. 2. The diameter of pipes which connect the VTPS and other installations in the flow loop are 50 mm. The geometrical details of the VTPS, made of plexiglass, are illustrated in Fig. 1, the pipe with the guide vanes installed near the inlet is 75 mm in diameter and 520 mm in length. At the other end of this pipe, a 200-mm long conical pipe, with four even distributed and tangentially holes in each cross section, connects it into the flow loop. The conical pipe is inside a 120 mm diameter concentric tube. A 50 mm diameter pipe located at the right top perpendicular to the concentric tube is used as the water-rich outlet.

During the experiments, water and oil phases are first pumped from the water and oil tanks respectively, mixed at the Y-junction and then this mixture fluid is sent to the VTPS. Through the centrifugal separation in VTPS, the tangential velocity is gained by the guide vanes at the inlet and thus a central symmetry swirl motion is formed. In the swirl motion, oil and water phases are separated due to density difference. Oil phase is mainly distributed around the pipe central axis while water phase moves towards the wall. And then, a water-rich stream exits from the tangentially drilled holes into the water-rich outlet and an oil-rich stream ejects through the centered upflow outlet. Finally both phases are pumped to the mixture tank for gravity separation and re-circulation.

2.2. Control and data acquisition systems

The LP-14 white oil and deionized water are used in the experiments, and their physical properties under test conditions (the atmosphere temperature is about 17 °C) are as follows: $\rho_o = 836.0$ kg/m³, $\mu_o = 0.245$ kg/m s, $\rho_w = 1000.0$ kg/m³, $\mu_w = 0.001$ kg/m s. The oil volume fraction at the inlet ranges from 2.0 to 20 percent.

The oil and water pumps are variable frequency pumps which could alter the running speed to control the flow rates of oil and water respectively. The flow rate at the water-rich outlet is changed by the butterfly valve and measured by an ultrasonic flowmeter. The flow loop is also equipped with several pressure transducers for pressure measurement. All output signals from the sensors are collected at a central data-acquisition panel. The oil concentration in the separated water
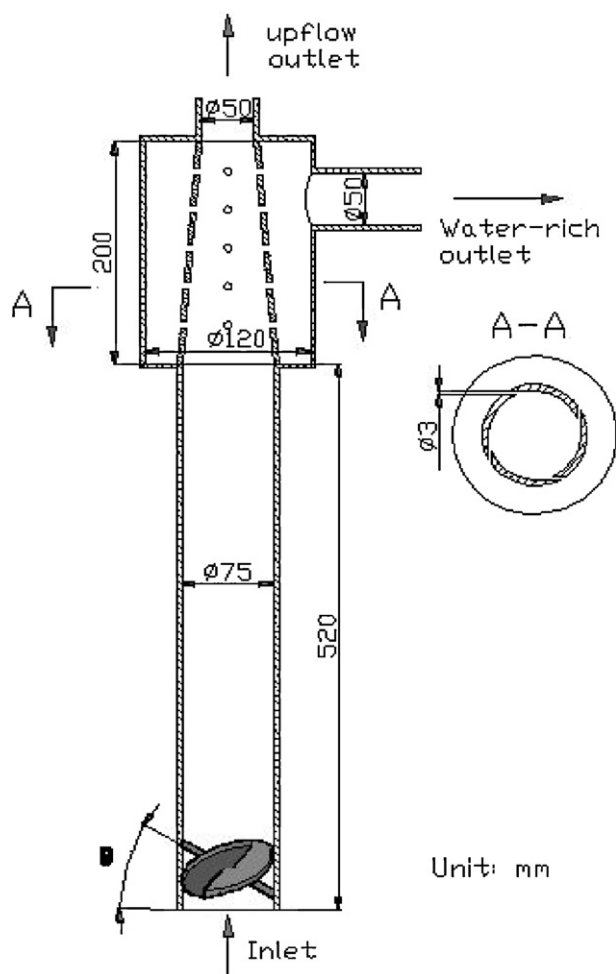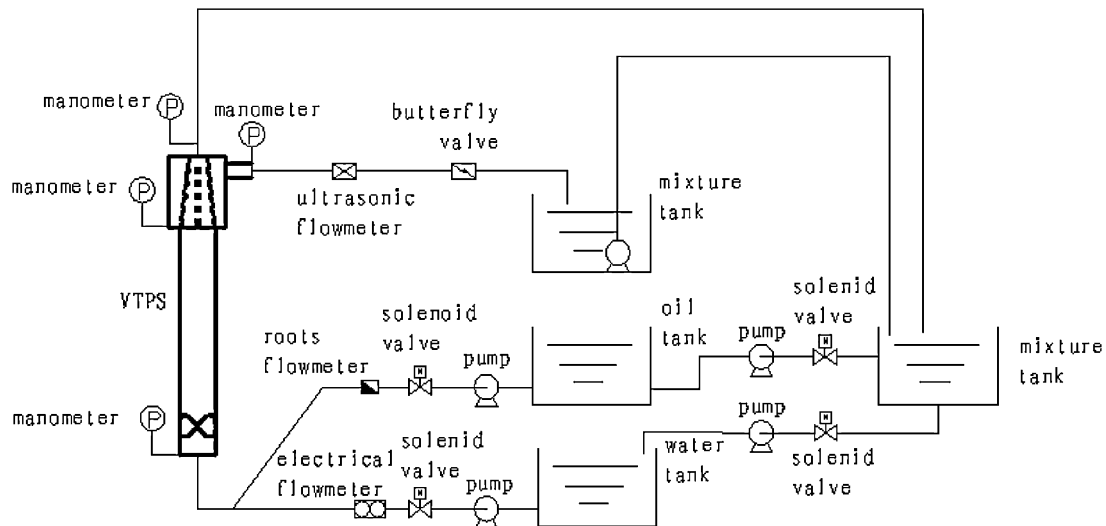
to separate oil phase from water by getting rid of reverse flow in dynamic hydrocyclones. In the vortex flow field of dynamic hydrocyclones, water moves toward the wall, and then drains from the side outlet, while oil phase is forced to the center, and ejected through the centered oil outlet (Standridge et al., 1999). Their experiments showed that such improvement performed better than the traditional hydrocyclones. But as the downhole pressure is always very high, it is a problem to seal up the dynamic hydrocyclones and the separated-water is likely to be re-mixed with the liquid at the inlet.

The above literature review reveals a contradiction between the practical needs and limitation of hydrocyclones which is mainly caused by their inlet structure (tangential inlet in the narrow wells making their scale limited and that confining the efficiency) and their diverse flow direction between the inner and outer rotation flow. In view of this problem, inspired by the gas–liquid axial separator designed by Swanborn (Swanborn, 1988; Delfos et al., 2004), a new kind of vane-type pipe separator (VTPS) is proposed in this work and the structure of a VTPS is shown in Fig. 1. The designs base on the idea of symmetrical flow field and decrease the crisis of oil phase to be re-injected. Thus the static guide vanes and tangentially drilled holes are designed. This VTPS for oil–water separation is a kind of axial flow cyclone and has some advantages in the aspects of separation performance as followings: Firstly, there is no slender cone and tangential inlet so that the VTPS has a low-pressure drop and a relative larger volume for oil–water separation (Standridge et al., 1999) which makes it quite suitable for the downhole oil–water separation; Secondly the diameter of

Fig. 2 – Flow loop of experimental system.

phase is measured by OilTech 121A Handheld Oil in Water Analyzer with the measurement accuracy within 5 ppm.

2.3. Experimental arrangement

For VTPS, the guide vanes are the key component to form swirl flow field. In this study, the effect of their installation angle θ and number n on oil–water separation performance is discussed. Table 1 shows the five designs and the thickness of guide vanes are 2 mm.

3. Velocity field distribution

To measure the cross-sectional distribution of velocity field downstream of the guide vanes, a two-dimensional particle image velocimetry (2D PIV) is employed. The PIV system is produced by Germany LaVision company. The light source is a double pulsed Nd:YAG laser that sends short duration (4 ns) high energy (800 mJ) pulses of green light (532 nm). The collimated laser beam transmitted through one adjustable lens and two concave cylinder lens to generate a 1 mm thick light-sheet and illuminate the flow of a plane. The light reflected by the tracer particles (10 μm in average size, 1000 kg/m^3) which is evenly distributed in water is recorded at 5 Hz by a CCD camera with 1376 × 1040 pixels. Images are formed through the imaging array. The analysis of the images is processed by adaptive correlation (Davis 7.2 Software) which gives a 64 × 64 vectors grid on 32 × 32 pixel-size final interrogation spots and the pixel resolution is 6.45 × 6.45 μm. Through the adaptive correlation, the location $x(t)$, $y(t)$ of the same tracer particle are functions of time t. So the velocity of water point that the tracer particle locates can be expressed as follows:

$$v_x = \frac{dx(t)}{dt} \approx \frac{x(t + \Delta t) - x(t)}{\Delta t} = \overline{v_x} \tag{1}$$

$$v_y = \frac{dy(t)}{dt} \approx \frac{y(t + \Delta t) - y(t)}{\Delta t} = \overline{v_y} \tag{2}$$

here v_x, v_y are the instantaneous velocity along the x direction and y direction respectively; $\overline{v_x}$, $\overline{v_y}$ are the mean velocity along the x direction and y direction respectively; Δt is the time interval between the two continuous shooting.

PIV system can obtain velocity vector of the entire planes and is proved to be an effective test method. Lim et al. (2010) adopted 2D PIV to study the velocity vector distributions within the hydrocyclone. Martins et al. (2010) compared the typical behaviour of the tangential and axial mean velocity components got by both LDA (Laser Doppler Velocimetry) and 2D PIV. They found a good agreement between the two methods.

During this experiment, to minimize the effects of reflection and refraction of the light beams, a water cube tank is placed surround the VTPS. The averaged (100 samples in 20 s) flow field of the cross section and axis cross-section in a VTPS with 4 guide vanes at θ of 30° is shown in Fig. 3. The axial velocity profile could be obtained is from the averaged flow field of axis cross-section, while the tangential velocity profiles is acquired from averaged flow field of cross-section.

Fig. 4 gives the axial and tangential velocity profile in the VTPS where the axial distance from the guide vanes is double of the pipe's diameter when the flowrate of water at the inlet is 12.00 m^3/h. The axial velocity has no zero vertical velocity, which means that there does not exist axial reverse flow. Thus, this structure reduces the remix between the oil core in the center area and water phase in the surrounding area. Another characteristic of axial velocity profile is that the maximum value appears in the center area, which helps to prevent the oil droplet in the center area from flowing into the water-rich stream in the cone section. However, in the hydrocyclone, the axial velocity near the wall is negative and positive in the center area. This induces that the maximum axial velocity in the center area is larger in the VTPS than the hydrocyclone. Therefore, the VTPS performs better than the hydrocyclone for its rapid moving the oil phase into the center area. From the tangential velocity distribution, it is a central symmetric vector field. In a word, the flow field distribution in the VTPS is better for oil–water separation.

4. Results of separation performance and discussion

4.1. Effects of split ratio

To investigate the effect of the split ratio on oil–water separation in the VTPS, experiments were carried out with θ of 20° and the same guide vanes' number of 3.
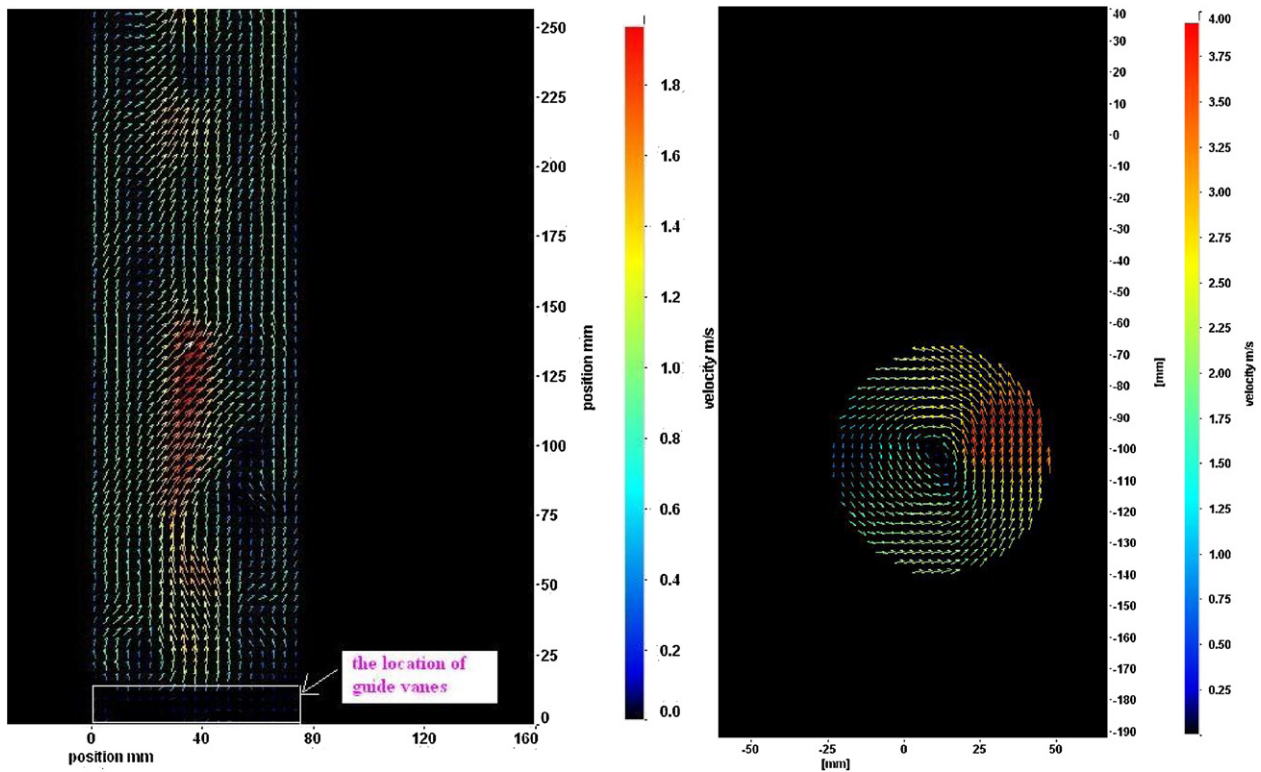
Fig. 3 – The averaged velocity field of the axis cross section (left) and cross section (right) in the VTPS.

Split ratio is defined as:

$$F = \frac{Q_w}{Q_i} \tag{3}$$

where Q_w is the flowrate at the water-rich outlet, Q_i represents the flowrate at the inlet.

Fig. 5 shows the effect of split ratio on the distribution of oil and water phases in the VTPS. The gray in the center of VTPS represents oil phase. When the flowrate is 3.53 m³/h, the oil content is 8.0% at the inlet. It can be seen that as the

increasing of split ratio, the diameter of oil core in the VTPS enlarges. Fig. 6 gives the effect of split ratio on both the oil content at the water-rich outlet and the water content at the upflow outlet. The curve in diagram shows that the oil content at the water-rich outlet increases with the increasing of split ratio. It means that there exists a critical split ratio to re-inject this water-rich mixture within the reinjection standard into the ground. In this experiment, the water content at the upflow outlet reaches 40.1% with oil concentrations in the separated water phase of less than 250 ppm. This value shows that the VTPS performs better than the typical hydrocyclone
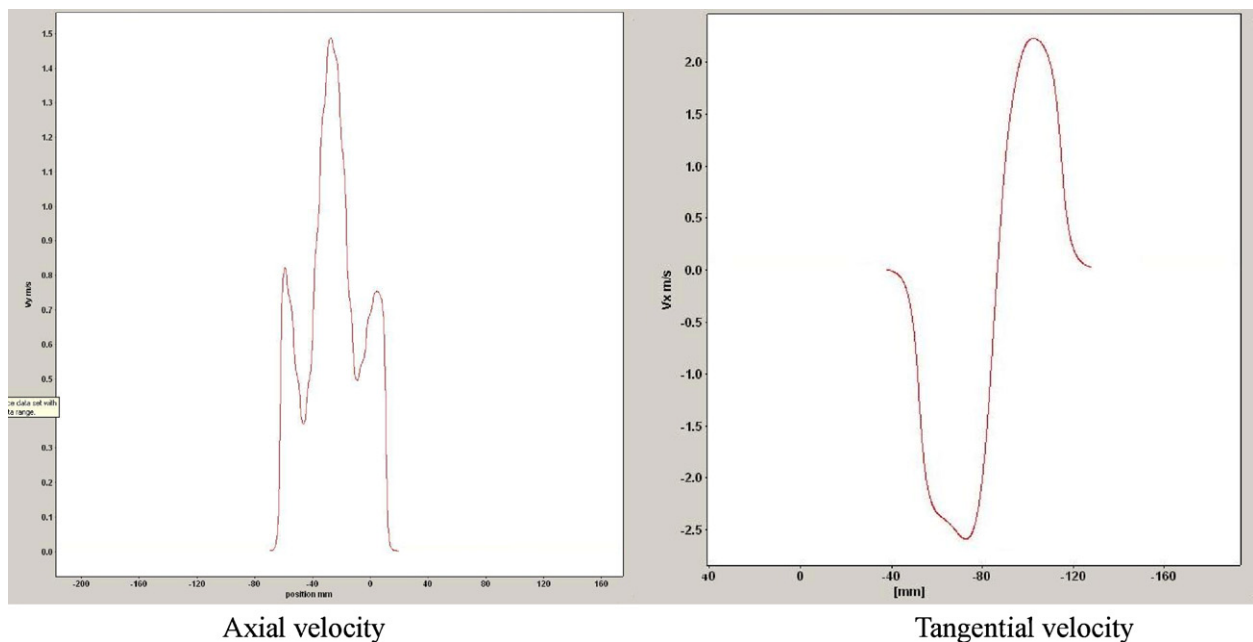

Axial velocity   Tangential velocity

Fig. 4 – The tangential and axial velocities profiles in the VTPS.

F=0.00   0.06   0.19   0.35   0.81   0.867
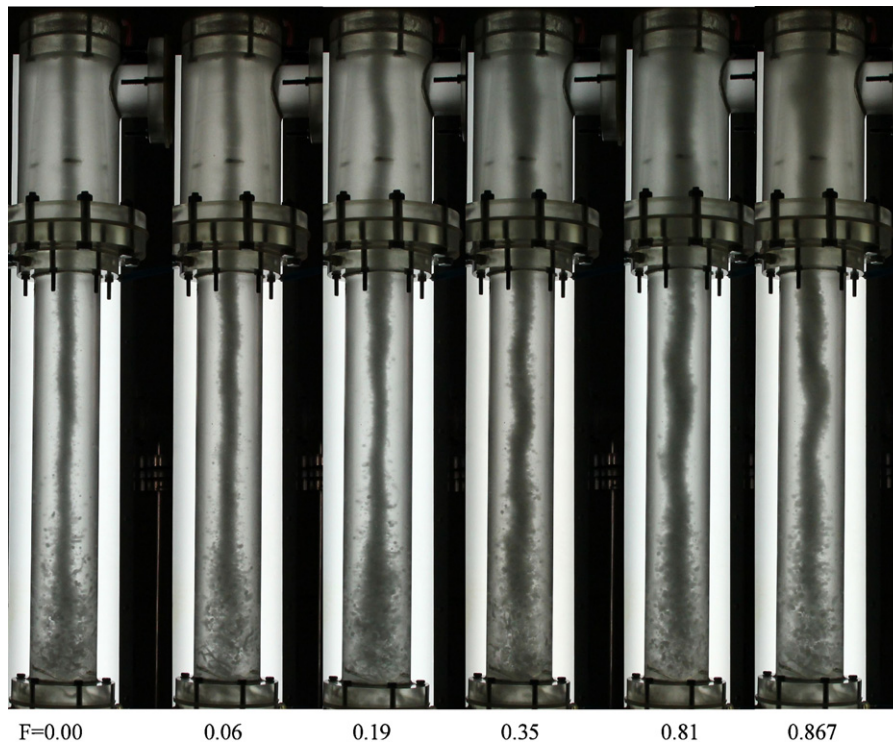
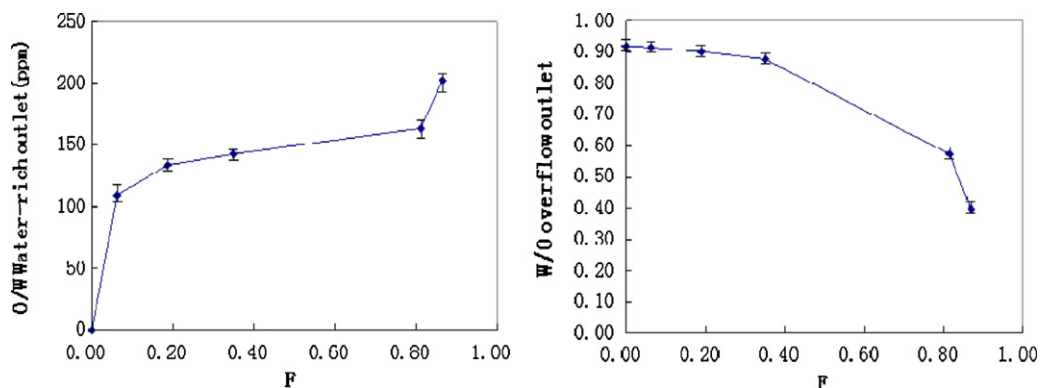**Fig. 5 – Distribution of oil and water in the VTPS under different split ratio.**

Fig. 6 – Effect of split ratio on oil–water separation performance.

in which the water content at the overflow of 50.0–67.0% with oil concentration in the separated water phase of 100–500 ppm (Klasson et al., 2005).

4.2. Effects of the oil content

Fig. 7 shows the effect of oil content on purifying in VTPS with θ of 20° and the same guide vanes' number of 3 under different split ratio. Fig. 8 shows the effect of oil content on distribution of oil and water in the VTPS at zero split ratio.

As shown in Fig. 7, when the flowrate at the inlet is 4.07 m³/h and the split ratio is smaller than 0.40, with the increase of the oil content at the inlet, the oil content at the water-rich outlet decreases firstly, and then increases. According to the experimental observation shown in Fig. 8, when the oil content is small, the oil phase entering the inlet of the VTPS are dispersed more small balls. When the oil content increases, the oil phase is scattered as churns and the average diameter of droplet after the break-up in VTPS is larger. So the oil content at the water-rich outlet decreases first and then increases because the diameter of oil core increases quickly as the oil content at the inlet is greater than 6.0%.

From Figs. 7 and 8, it is observed that when the oil content arrived at 20.1%, the oil content at the water-rich outlet is within 400 ppm with the split ratio of 0.70. It means that the VTPS could be used in wells with water content of 79.9% which seems an exciting result compared to the hydrocyclone using in wells with water content of more than 88.4%.
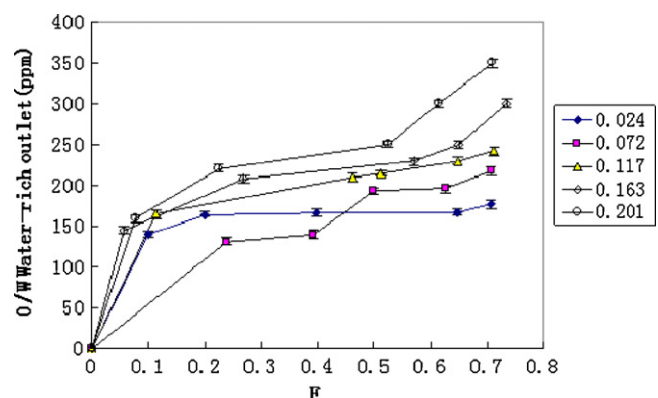

Fig. 7 – Effect of oil content on purifying in the VTPS under different split ratios.
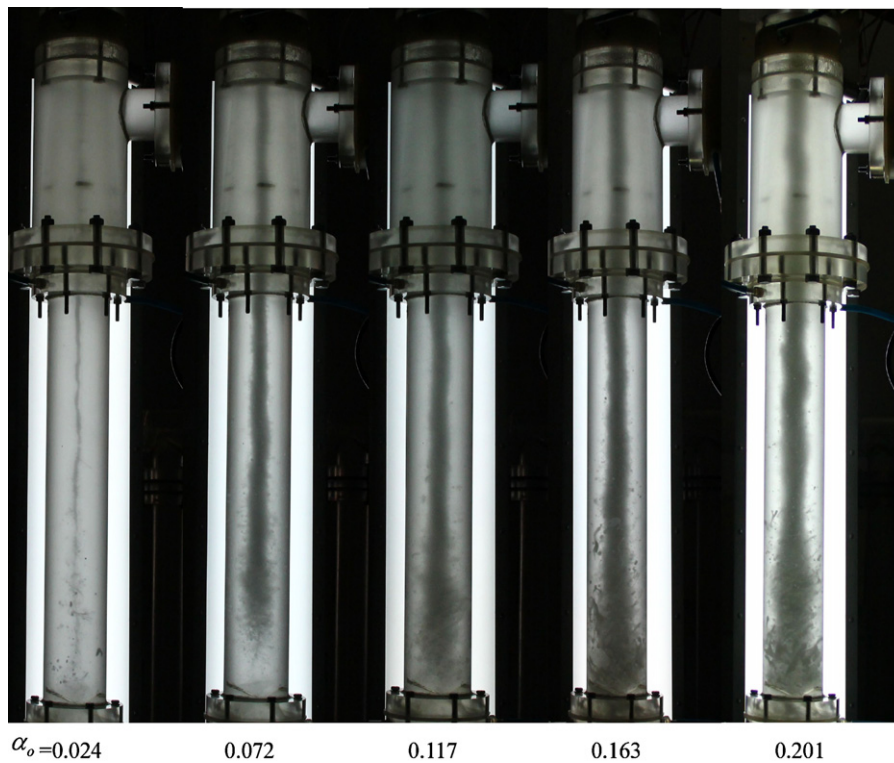
Fig. 8 – Distribution of oil and water at different oil contents.

4.3. Effects of guide vanes' installation angle

For the VTPS, the installation angle of guide vanes is another important geometric parameter for influences on the oil–water separation. To illustrate this, some experiments were discussed under the same flow rate at the inlet and the same guide vanes' number of three in the VTPS.

Fig. 9 shows the effect of guide vanes' installation angle on the oil and water distribution in the VTPS with zero split ratio.

It can be found that when the flowrate is 4.07 m^3/h and the oil content is 2.4% at the inlet, as the installation angle increases, the average droplet diameter in VTPS increases and so does the diameter of oil core.

Fig. 10 shows the effect of different guide vanes' installation angle on purifying after oil–water separation in VTPS with different split ratio. It could be observed that when the split ratio is below 0.10, the installation angle of 40° has the best result because the concentration of oil in water at the water-rich outlet is the smallest among these three designs. When the split ratio is large than 0.10, the VTPS with installation angle 30° has the least oil cut at the water-rich outlet. From Fig. 9, it could be found that at the same condition, as the decrease of the guide vane's angle, the smaller the oil droplet increased. The droplet in VTPS is too small to be separated from water. When the guide vane's angle is too large, the tangential velocity diverted is not very large. Although the oil droplet is large, the vortex formed by the tangential velocity is not strong enough to separate the mixture fluid. So when the flow rate at the inlet is 4.00 m^3/h, the VTPS with guide installation angle of 30° is the best.

4.4. Effects of guide vanes' number

Figs. 11 and 12 show the number of guide vanes' effect on oil–water separation in VTPS with the same θ of 30°. When the mixture flowrate at the inlet is 7.30 m^3/h and the oil volume fraction is kept at 2.4%, the distribution of oil and water phases in VTPS with $F = 0$ is presented in Fig. 11. It indicates that as the number of guide vanes increases, the axial distance for the oil droplets moving to the centre area is shorter.
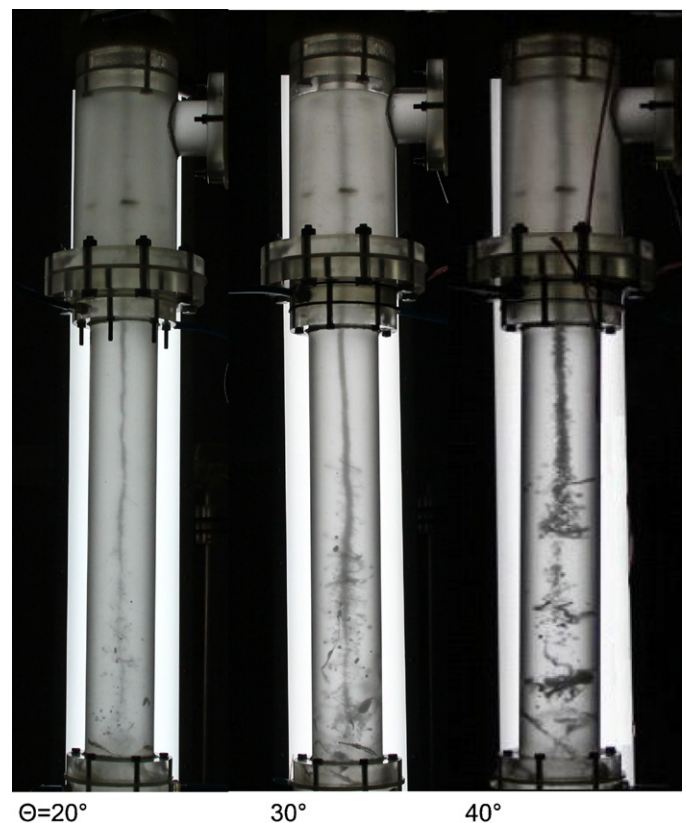

Fig. 9 – Distribution of oil and water in the VTPS with different guide vane's installation angles.
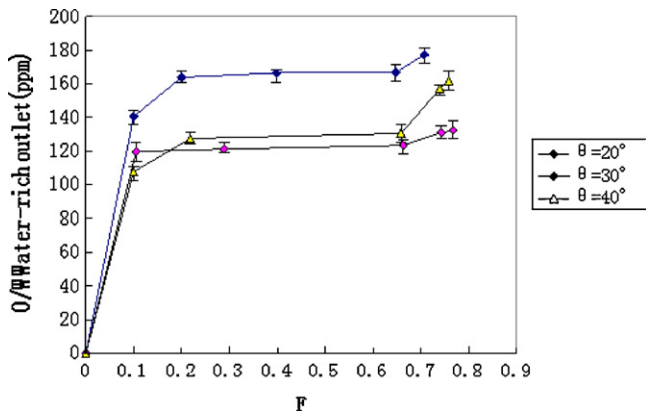
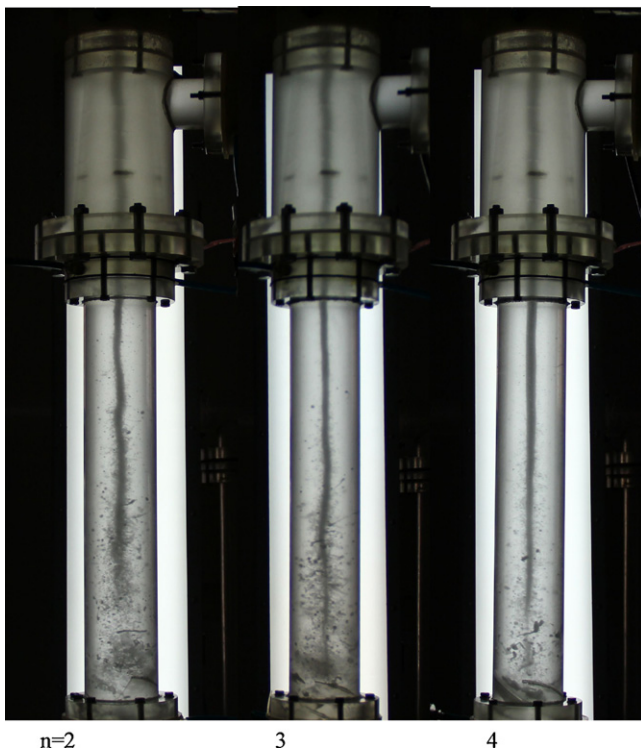**Fig. 10 – Effect of guide vanes' installation angle on purifying.**

n=2   3   4

Fig. 11 – Distribution of oil and water in the VTPS with different guide vane's numbers.
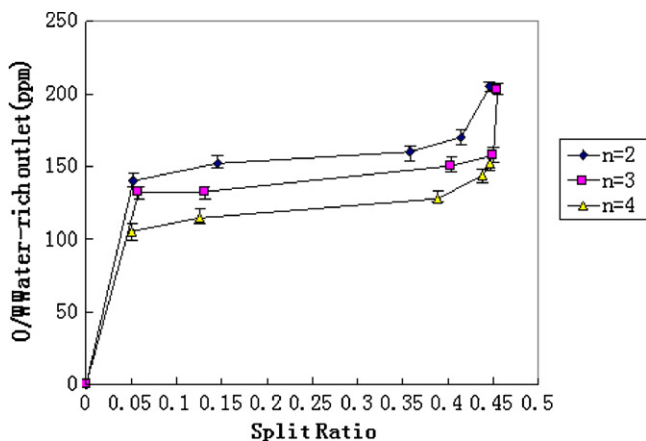

Fig. 12 – Effect of guide vanes' number on purifying.

Fig. 12 shows the oil volume fraction at the water-rich outlet of VTPS with different guide vanes' number when the split ratio increases. As can be observed that the oil content at the water-rich outlet decreases with the increases of guide vanes' number under the same split ratio. Increasing the number of guide vanes means more mixture fluid converted by the guide vanes to improve the average tangential velocity of the fluid. The force on a small droplet in this flow could be assumed to abide by Stokes law (Bird et al., 1960). The radial velocity is calculated through a balance between the Stokes drag and the centrifugal force on another reasonable assumption that the dispersed phase has the same axial and tangential velocity as the continuous phase (Frans et al., 1995):

$$\frac{4(\rho_w - \rho_0)\pi D^3 v_\theta^2}{3\pi} = 6\pi v \rho_o D \frac{dr}{dt} = 6\pi v \rho_0 D v_r \tag{4}$$

where D is the nominal diameter of oil droplet; ρ_w and ρ_o are the densities of oil droplet and water; v_θ is the tangential velocity; r is the revolving radius of the droplet in VTPS; v is the kinematic viscosity; v_r is the radial velocity.

It is implied that under the same other conditions, the radial velocity of the oil droplet is proportional to the tangential velocity and the size of the droplet. When the inlet flow rate is not very large, the more the guide vanes, the more strong tangential flow are converted from the axial flow at the inlet. As a result, the average tangential velocity is larger and the radial velocity of the oil droplet moving is faster. The oil droplet takes shorter time to move into the central area and the diameter of oil droplet which migrates into the central area within the same time is smaller. At the same rest conditions, as the number of guide vanes increases, the oil volume fraction at the water-rich outlet decreases.

5. Conclusion

In this work, two-dimensional flow in a new type of oil–water separator (VTPS) for the possible downhole applications has been characterized through the PIV techniques. The characteristics of tangential and axial velocity profiles have been acquired and show a new thought of oil–water separator.

The water content at the oil-rich stream after the separation in VTPS can reach is lower than the typical hydrocyclone, thus the separation efficiency is higher. Besides, VTPS has a wide working oil content range up to 20.1% and compact structure which has the possibility to handle a large amount of produced liquid downhole.

As the increase of split ratio, the oil-content in water-rich stream raises and is beneficial to the oil–water separation in VTPS. But too large a split ratio will lead to a certain amount of oil to be drained in to ground, so a critical split ratio exists when the oil-content in the water-rich stream reaches the reinjection standard.

The installation angle and number of guide vanes affects the diameter of the oil droplets distribution and the converted tangential velocity in VTPS. Under the same testing conditions and the designs in this work, installation angle of 30° is the optimum and four guide vanes are the best.

References

Bird, R.B., Stewart, W.E., Lightfoot, E.N., 1960. Transport Phenomena. Wiley, New York, 59.

Bowers, B.E., Brownlee, R.F., Schrenkel, P.J., 1999. Development of a downhole oil/water separation and reinjection system for offshore application. SPE Prod. Facilities 15 (2), 115–122.

Chapuis, C., Lacourie, Y., Lancois, D., 1999. Testing of Down Hole Oil/Water Separation System in Lacq Superieur Field. France, SPE Paper, No. 54748.

Delfos, R., Murphy, S., Stanbridge, D., Olujic, Z., Jansens, P.J., 2004. A design tool for optimising axial liquid–liquid hydrocyclones. Miner. Eng. 17, 721–731.

Frans, T.M., Nieuwstadt, Dirkzwager, Maarten, 1995. Fluid mechanics model for an axial cyclone separator. Ind. Eng. Chem. Res. 34, 3399–3404.

Jiang, M.-h., Zhao, L.-x., Wang, Z., 2002. Effects of geometric and operating parameter on pressure drop and oil–water separation performance for hydrocyclones. In: Proceeding of The Twelfth International Offshore and Polar Engineering Conference, Kitakyushu, Japan, May 26–31, pp. 102–106.

Klasson, K. Thomas, Taylor, Paul A., Walker Jr., Joseph F., Jones, Sandie A., Cummins, Robert L., Richardson, Steve A., 2005. Modification of a centrifugal separator for in-well oil–water separation. Sep. Sci. Technol. 40, 453–462.

Lim, Eldin Wee Chuan, Chen, Y.-r., Wang, C.-h., Wu, R.-m., 2010. Experimental and computation studies of multiphase hydrodynamics in a hydrocyclone separator system. Chem. Eng. Sci. 65, 6415–6424.

Listewnik, J., 1984. Some Factors Influencing the Performance of De-Oiling Hydrocyclone for Marine Applications.Second International Conference on Hydrocyclones, England, September 19–21.

Martins, L.P.M., Duarte, D.G., Loureiro, J.B.R., Moraes, C.A.C., Silva Freire, A.P., 2010. LDA and PIV characterization of the flow in a hydrocyclone without an air-core. J. Petrol. Sci. Eng. 70, 168–176.

Matthias Meyer, Matthias Bohnet, 2003. Influence of entrance droplet size distribution and feed concentration on separation of immiscible liquids using hydrocyclones. Chem. Technol. 26, 660–665.

Michdet, J.F., Sangesland, S., 1996. Downhole separation of oil and water. In: The 9th Underwater Technology Conference, Bergen, Norway, March 20–22.

Ogunsina, O.O., Wiggins, M.L., 2005. A Review of Downhole Separation Technology. SPE Paper, No. 94276.

Schutz, S., Gorbach, G., Piesche, M., 2009. Modeling fluid behavior and droplet interactions during liquid–liquid separation in hydrocyclones. Chem. Eng. Sci. 64, 3935–3952.

Sooran, N., Hassan, S., Hashemabadi, 2009. CFD simulation of inlet design effect on deoiling hydrocyclone separation efficiency. Chem. Eng. Technol. 32 (12), 1885–1893.

Standridge, D., Swanborn, R., Olujic, Z., 1999. A novel recycle axial flow cyclone with strongly improved characteristics for high-pressure and high-throughput operation. Multiphase, 555–563.

Swanborn, R.A., 1988. A new approach to the design of gas–liquid separators for the oil industry, Ph.D. Thesis, Delft University of Technology.

Thew, M.T., 1986. Hydrocyclone redesign for liquid–liquid separation. Chem. Eng., 17–23.

van den Broek, W.M.G.T., van der Zande, M.J., Janssen, P.H., 2001. Downhole dehydration vs.reduction of oil droplet break-up. SPE Paper, No. 66542.

Veil, John A., Langhus, Bruce G., Belieu, Stan, 1999. DOWS reduce produced water disposal costs. Oil Gas J. March, 76–85.

Zhao, L.x., Li, F., Ma, Z.-z., Hu, Y.-q., 2010. Theoretical analysis and experimental study of dynamic hydrocyclones. ASME 132 (042901), 1–6.